

# Antenna Gain Calibration with Improved Accuracy Modeling of Pyramidal Standard Gain Horns, Part 2

Domenic Belgiovane, *Member, AMTA*  
MVG - Orbit Advanced Technologies, Inc.  
650 Louis Dr, Warminster, PA, USA  
domenicb@orbitfr.com

Justin Dobbins *Fellow, AMTA*, Afifeh Khatabi  
Raytheon Technologies  
1151 E Hermans Rd., Tucson, AZ, USA  
{justin.dobbins,afifeh.khatabi}@rtx.com

Andrea Giacomini, *Senior Member, AMTA*, Francesco Saccardi, *Fellow, AMTA*, Lars J. Foged *Fellow, AMTA*  
Microwave Vision Italy  
Via dei Castelli Romani 59, Pomezia, Italy  
{andrea.giacomini,francesco.saccardi,lars.foged}@mvg-world.com

**Abstract**—This is a continuation of the work presented at the AMTA 2022 symposium to assess the accuracy of on-axis antenna gain with commercially available computational electromagnetic (CEM) solvers [1]. Common practice for computing antenna gain normalization via the gain-transfer technique is to use the on-axis NRL gain curve of a pyramidal standard gain horn (SGH) derived by Schelkunoff and Slayton [2], [3]. Due to approximations in this formulation, Slayton assessed an uncertainty of  $\pm 0.3$  dB for typical SGHs operating above 2.6 GHz. Since this uncertainty term is often one of the largest terms in the range measurement uncertainty budget for AUT gain, it is highly desirable to reduce it. Many studies in the past have attempted to improve upon Slayton’s expressions for SGH gain, but none have achieved widespread use. The previous investigation demonstrated the use of several commercially available solvers, including HFSS™, CST Studio Suite®, and FEKO® to model the on-axis directivity and gain of a commercial off-the-shelf (COTS) X-band SGH [1]. In that work, the CEM simulation results from multiple solvers in HFSS™, CST Studio Suite®, and FEKO® are shown to be within  $\pm 0.0075$  dB of each other. This work is an extension to study how closely the simulation models match recent measurements of gain for the same MVG SGH820 horn discussed in previous paper. These measured and modeled results are compared with the international intercomparison results of a similar SGH [4], in conjunction with a best-estimated simulation model of the original dimensions from [4]. To capture the differences of the physical as-built antenna versus the simulation model, a simple tolerance study in simulation is performed based on the build tolerances of the antenna to provide an uncertainty estimate of the simulation results.

## I. INTRODUCTION

THIS work further investigates the use of simulated on-axis gain values for the pyramidal standard gain horn (SGH) geometry [2], [3] that is commonly used in the gain transfer (aka gain substitution, gain comparison) method for determining the unknown gain of an antenna under test (AUT) [5]. Building upon the simulation-only results presented in [1], this work uses the same simulation methodology to predict the gain of another X-Band SGH with previously published results from measurement [4], and compares the previous simulation results from [1] against new measurements of the SGH820. The comparison of simulations and measurements establishes a baseline level of confidence for

the simulation approach, and highlights some areas for further investigation. This work also includes a more rigorous assessment of some of the uncertainty terms introduced in Table II of [1]. Specifically, this work addresses the gain uncertainties associated with the differences in the physical vs. modeled dimensions of the SGH. After presenting these results, we re-assess the uncertainties of the proposed modeling method against the industry-standard value of  $\pm 0.3$  dB for typical SGHs operating above 2.6 GHz [3].

## II. MODELING METHODOLOGY

The primary goal of the modeling methodology in this paper is to determine, to the best of our ability, the on-axis gain variations due to manufacturing variability. To achieve this, a tolerance analysis has been completed in simulation based on the manufacturing drawing. In a similar manner to the companion paper [1], the pyramidal SGH was modeled in multiple major commercial CEM tool suites: HFSS™ from Ansys® and CST Studio Suite® from Dassault Systemes. As was shown in [1], all commercial CEM tools and respective solver variants achieved extraordinary intercomparison accuracy withing  $\pm 0.0075$  dB of each other. Hence, if properly modeled there is an extremely high degree of confidence that the results are comparable no matter which tool is used.

Originally before the days of modern computing and CEM techniques, the SGH gain curve was computed analytically with a geometric optics solution. This derivation neglects diffraction terms at the horn aperture. As previously discussed, this approach is still commonly used today and it useful for a first-order solution to the SGH. To compare the CEM modeling and measurements against the NRL curves, the gain of the SGH can be estimated from [3], as:

$$g = \frac{8\pi l_e l_h}{ab} [C^2(w) + S^2(w)] \times \left[ \{C^2(u) - C^2(v)\}^2 + \{S^2(u) - S^2(v)\}^2 \right] \quad (1)$$

where

$$u = \frac{1}{\sqrt{2}} \left( \frac{\sqrt{\lambda l_h}}{a} + \frac{a}{\sqrt{\lambda l_h}} \right), \quad v = \frac{1}{\sqrt{2}} \left( \frac{\sqrt{\lambda l_h}}{a} - \frac{a}{\sqrt{\lambda l_h}} \right),$$

$$w = \frac{b}{\sqrt{2\lambda l_e}},$$

and  $\lambda$  is the wavelength. The variables  $l_e$ ,  $l_h$ ,  $a$ , and  $b$  are shown in Figure 1. The well-known Fresnel integrals are represented by  $C(x)$  and  $S(x)$ .

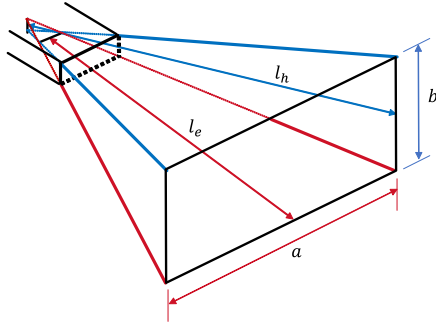


Fig. 1. Interior dimensions of NRL Type Standard Gain Horn Antenna.

### A. CEM Simulation Methodology

As previously shown [1] there are many different options for full wave solvers. This section will discuss the various implementations and nuances of these CEM solution methods as they pertain to presented model results of this paper.

In this paper, the X-band NRL type SGH [3] is studied from the original Scientific Atlanta (SA) Model 12-8.2 as well as the Microwave Vision Group (MVG) SGH820. These two antennas were intended to have the same internal geometries, but in reality they have slight differences. The nominal dimensions for both antennas as well as the maximum and minimum dimensional tolerances are listed in Table I with dimensional variables annotated in Figure 2.

TABLE I  
DIMENSIONS OF THE SGH FOR THE TOLERANCE STUDY ACROSS CEM TOOLS WITH UNITS IN INCHES.

	MVG Nominal	SA Nominal	Min Tolerance	Max Tolerance
$a_{wg}$	0.90000	0.90000	-0.005	+0.005
$b_{wg}$	0.40000	0.40000	-0.005	+0.005
$L_{wg}$	1.33071	2.59000	-0.060	+0.060
$t_{wall}$	0.07874	0.12500	-0.010	+0.010
$a$	7.65354	7.65400	-0.040	+0.040
$b$	5.66929	5.66900	-0.040	+0.040
$L_{horn}$	11.4091	11.4100	-0.060	+0.060
$t_{wg}$	0.07874	0.05000	-0.008	+0.008

These tolerances are a representative worst case for both antennas and their manufacturing drawings. The SA Model 12-8.2 was chosen due to the extent of which it has been studied in the international X-band horn intercomparison [4].

For the SA model 12-8.2 some assumptions had to be made because the exact details of the gold standard calibration antennas at NIST for SN 1 and 2 are not precisely known. Furthermore, the authors found that while all SA, MI Technologies, and NSI-MI drawings have consistent dimensions over decades of manufacturing history, the dimensions used in at least two publications are off-nominal but within allowable manufacturing tolerances [6], [7]. The authors also found

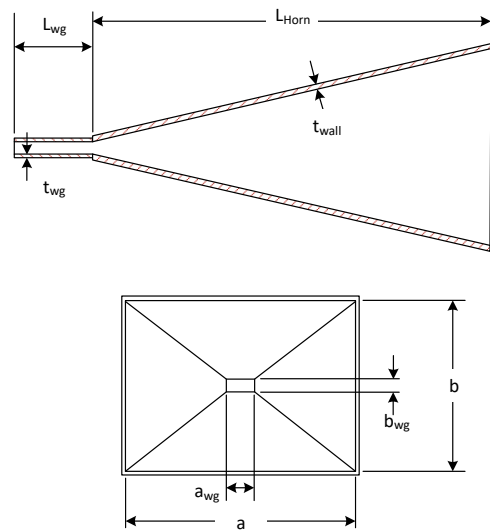


Fig. 2. Dimensions of Standard Gain Horn Antenna used for the tolerance study.

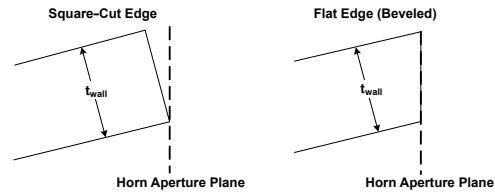


Fig. 3. Description of SGH aperture edge cut geometry.

evidence that the horn manufacturing methods changed over the years. For example, the SN 1 and SN 2 horns, which were likely manufactured in the early 1970's, were fabricated with the forward edge beveled to be perpendicular to the axis of the horn (parallel to the waveguide flange), shown in Figure 3 as the flat edge (or beveled edge), while later models of the same horn did not include that finishing step so the edges of the horn were square-cut sheet metal, shown in Figure 3 as the square-cut edge. The flat edge aperture geometry was assumed in the CEM model for each horn, with the exception of the high-fidelity model discussed later in this paper.

To assess the uncertainties associated with manufacturing tolerances, a CEM study was performed on both horns using the build tolerances in in Table I. To better model the gain of the antennas, as opposed to the directivity, the SGHs were assumed to be made completely out of aluminum. Although the specific implementation of material modeling can vary between each simulation solver, the same material properties were used across all simulations. The material properties for aluminum were taken from the materials library in the Ansys HFSS™ tool as  $\epsilon_r = 1$ ,  $\sigma_e = 3.8 \times 10^7$  S/m,  $\mu_r = 1.000021$ , and  $\tan\delta_\mu = 0$  with a measured frequency of 9.4 GHz.

### B. Simulation Results

The nominal designs of the MVG SGH820 and the SA Model 12-8.2, as described in Table I, were modeled using HFSS 2022 R2 FEM solver with higher-order basis functions. Both models were configured with electric and magnetic

symmetry planes. A PML boundary condition was applied for the radiation boundary with a vacuum box by using the PML setup wizard based on the model geometry of  $\lambda/8$  at 8 GHz. The results for the MVG SGH820 are the same as reported in the previous paper [1] for the HFSS simulation. It is important to note that in both the prior work and this work the SGH820 coax-to-waveguide adapter is neglected and a waveport excites each SGH with the respective waveguide length specified in Table I.

A length-based mesh criteria was placed on the horn outer and inner edges based on  $\lambda/20$  at 12 GHz to account for the diffraction at the edge of the horn and add additional precision. The gain of the two simulated models were overlaid and plotted to determine the difference in magnitude (dB) over frequency as illustrated in Figure 4. Overall, the comparison between the two geometries is very good with less than a 0.04 dB maximum difference.

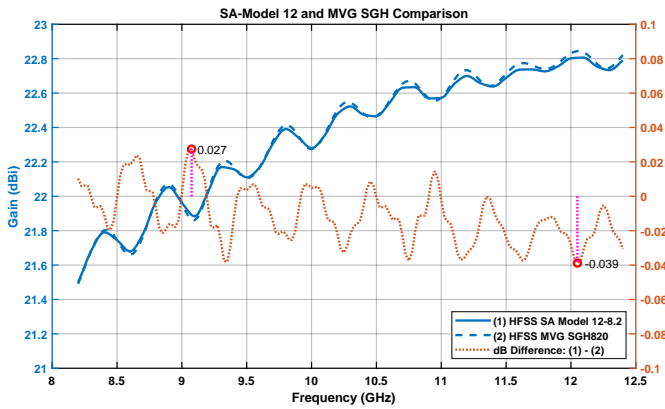


Fig. 4. Simulation comparison of the MVG SGH820 and SA Model 12-8.2 SGH antennas.

Next, the manufacturing tolerances from Table I were applied to the SA 12-8.2 SGH nominal dimensions of Table I. The simulation of each individual parameter and the maximum possible gain difference is shown in Figure 5. This bar chart was created by taking the maximum and minimum difference versus all frequencies from the nominal design.

From the chart it is clear that the length of the horn has the biggest impact on the uncertainty. Variations due to aperture edge shape (e.g., beveled vs. square-cut) are not shown here but initial studies suggest a non-negligible effect on the peak-to-peak ripple of the SGH frequency response.

A full Monte-Carlo analysis was not performed. To capture the effects considering all manufacturing tolerances, we set all of the variables from Table I to either a maximum or minimum value and compared against a model with all values set to nominal values. From these three simulations a maximum, minimum and mean value versus frequency was computed and compared in Figure 6.

Building on the modeling principles established in [1] as a baseline, the work in this section established uncertainty bounds for the contribution of manufacturing tolerances to the

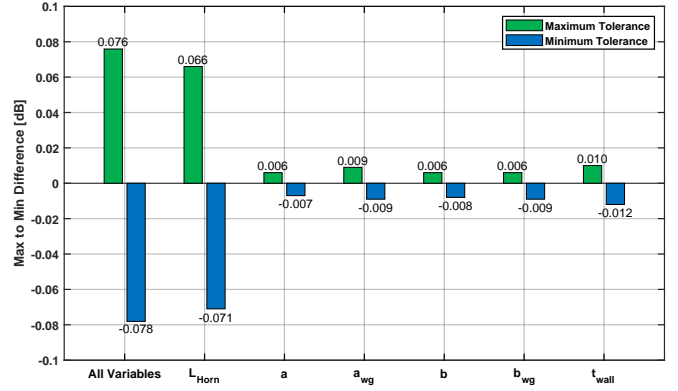


Fig. 5. Simulation comparison of individual tolerance variables of the SA Model 12-8.2.

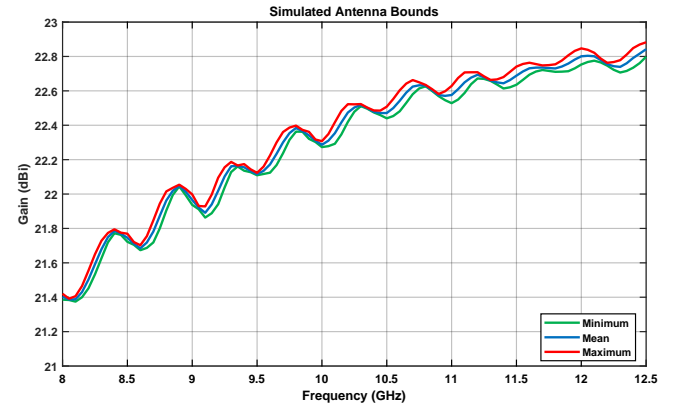


Fig. 6. Simulation comparison of the upper and lower bound tolerances for the SA 12-8.2 X-band SGH.

on-axis gain of the SGH. The next section of the paper will discuss the comparisons between simulation and measurement as well as the associated uncertainties of each.

### III. MEASUREMENTS OF THE SGH

This section discusses the measurements which have been performed on the previously described SGH antennas from SA and MVG. The well-known X-band intercomparison [4] was used as the reference, with on-axis gain measurements of the SA model 12-8.2 SGH SNs 1 and 2 re-plotted in Figure 7 with associated measurement uncertainty bars. The measured data from NIST and NPL were specifically chosen because they have uncertainty values associated with them. These uncertainty values of the measured data are shown in Table II.

The NIST curves in Figure 7 were measured in 1992 from 8.2 - 12 GHz with a published uncertainty ( $2\sigma$ ) of  $\pm 0.07$  dB across the whole band. The NPL curves were measured in 1991 with a published uncertainty ( $2\sigma$ ) of  $\pm 0.04$  dB from 8 - 10 GHz and  $\pm 0.07$  dB from 10 - 12.5 GHz. Both measurements used the three antenna extrapolation technique with the reference plane at the waveguide flange, meaning

TABLE II  
UNCERTAINTY OF ANTENNA MEASUREMENTS

Uncertainty Term	$2\sigma$ (dB)
NIST SA Model 12-8.2	$\pm 0.070$ dB
NPL SA Model 12-8.2 ( $< 10$ GHz)	$\pm 0.070$ dB
NPL SA Model 12-8.2 ( $> 10$ GHz)	$\pm 0.040$ dB
NPL MVG820	$\pm 0.090$ dB

the coax-to-waveguide adapter losses were not part of the measurement.

Generally all four curves in Figure 7 compare well especially at frequencies below 10 GHz. It becomes apparent that SN 2, shown with dashed lines, has less gain than SN 1 above 10 GHz. There's a clear divergence with the NIST data for SN 2 as well. This effect was not explained in [4], but it is assumed the the data for SN 1 is more representative of the nominal SGH design so it will be used as the measured SA Model 12-8.2 reference in the following sections.

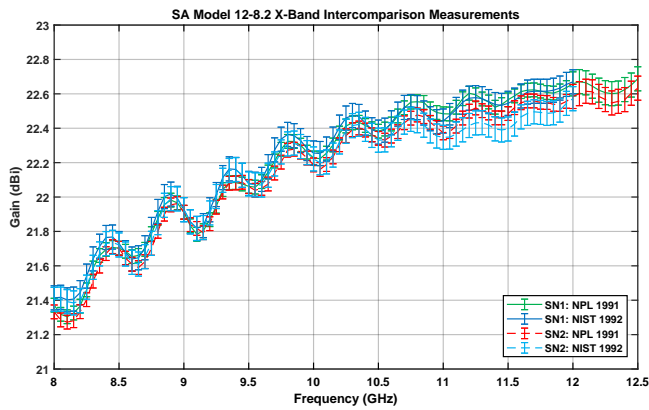


Fig. 7. Measurement of the Serial No. 1. and 2 SA Model 12-8.2 SGH antennas.

More recently in 2023, NPL performed on-axis gain measurements of an MVG SGH820 with an uncertainty ( $2\sigma$ ) of  $\pm 0.09$  dB. Figure 8 shows the comparison of the 1991 NPL measurements of the SA Model 12-8.2 with the 2023 MVG SGH820 measurements, where each curve is shown with its associated uncertainty bars.

Overall, there is fairly good agreement between the two different horn antennas. There are some slight geometric differences in the nominal dimensions as shown in Table I, so some variability is expected. Furthermore, since the SGH820 has an integrated coax-to-waveguide adapter, the 2023 measurements necessarily include that additional loss.

This section presented on-axis gain results for both the SA and MVG SGH antennas, as measured by industry-recognized calibration laboratories with the associated uncertainties in Table II. With this measured data, the next sections of the paper will compare simulations and measurements.

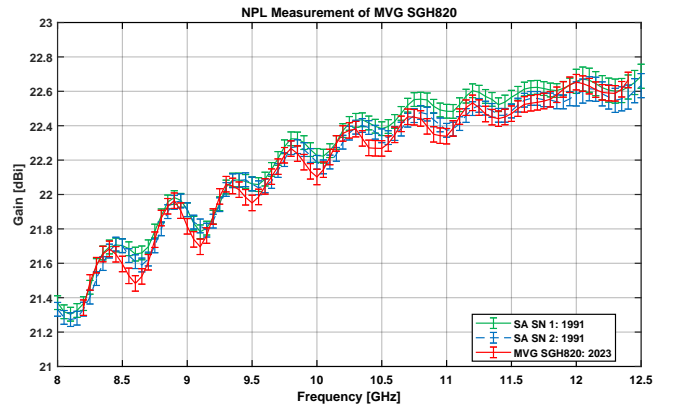


Fig. 8. NPL Measurement SA Model 12-8.2 compared to the MVG SGH820.

#### IV. UNCERTAINTY ANALYSIS

As previously discussed, the primary purpose of the tolerance study through CEM analysis was to assess the uncertainties associated with physical manufacturing variations. To determine the combined uncertainty with these variations, we build upon the uncertainty analysis from the previous paper [1], which are reproduced in Table III.

TABLE III  
LIST OF POTENTIAL SOURCES OF ERROR RELATED TO SIMULATION

Description of Error Term	Error
Coax-to-waveguide adapter	Measurable
Differences in Code Implementation [1]	$\pm 0.0075$ dB
Higher-order Waveguide modes	Negligible
Numerical Precision/Field Discretization	Negligible
Radiation Air Box Reflections	Negligible
Mesh Noise and Irregularities	Negligible
Differences in Physical vs. Model Dimension	$\pm 0.0781$
RSS Uncertainty	$\pm 0.0791$

Many of the terms are expected to be negligible, and the primary finding from [1] was that the inter-code differences had an uncertainty of  $\pm 0.0075$  dB. From the tolerance study in Section II the physical and model dimension differences were shown to be  $\pm 0.0781$  dB. The uncertainties for the coax-to-waveguide adapter proved difficult to quantify and will need to be studied in more detail later. Taking a root sum square (RSS) of the identified error terms, in linear units, the updated RSS uncertainty is  $\pm 0.0791$  dB. Of course, this uncertainty could be reduced with knowledge of the physical dimensions of a specific SGH that are easily obtained through mechanical inspection techniques such as a coordinate measuring machine (CMM). Note that because the maximum extents of manufacturing tolerances were investigated along with several different commercial CEM modeling tools, this combined uncertainty represents a worst-case value (i.e. 100% confidence interval). It should also be noted that the tolerances assume that the horn is completely symmetric. This was done so symmetry planes could be used in the modeling. In practice,

the horn could be slightly asymmetric. This variability was not studied in this work.

To demonstrate the modeling differences between Slayton’s equation in (1) and the CEM model of the SA Model 12-8.2 SGH with nominal dimensions, a comparison plot is shown in Figure 9.

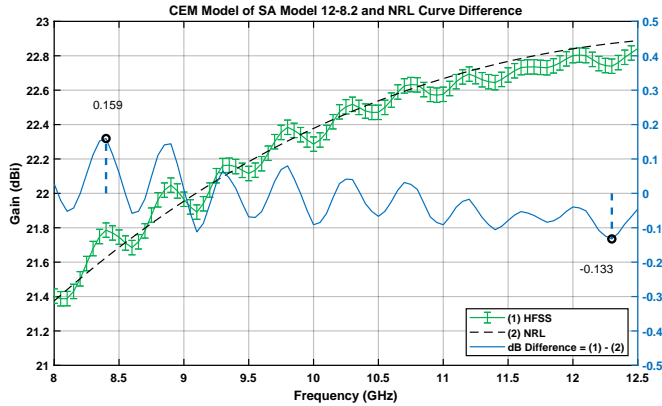


Fig. 9. Comparison of modeling difference of the SA Model 12-8.2 with the NRL gain curve from (1).

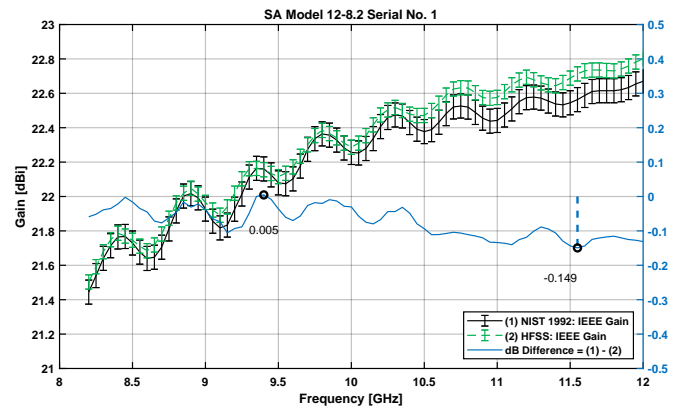
Overall, the CEM model has a maximum and minimum deviation of 0.159 dB and -0.133 dB, respectively, well below Slayton’s uncertainty bound of  $\pm 0.3$  dB. Slayton stated “In all probability, the actual errors are considerably less than the maximum possible tolerances quoted.” when referring to the error estimates of  $\pm 0.5$  dB below 2.6 GHz and  $\pm 0.3$  dB above 2.6 GHz [3]. Assuming the dimensions are known perfectly, the NRL curve predicts gain uncertainty (with no coax-to-waveguide adapter) within approximately  $\pm 0.16$  dB.

## V. COMPARISON OF MEASUREMENTS AND SIMULATIONS

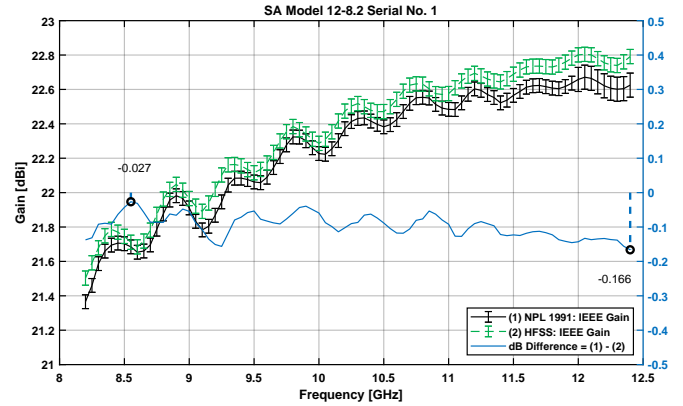
With the previously described measurements, CEM models, and uncertainty analysis, a quantified difference can be determined. The comparison of the SA Model 12-8.2 SN 1 measurements with the HFSS simulation is plotted in Figure 10 (a) for NIST and (b) for NPL.

Overall, there is a bias in the gain such that the simulated data is always higher than the measured data. Both comparisons are close to one another with the NIST measurements showing slightly better agreement at the highest frequencies. It is important to note that the measurements were performed with the calibration plane at the waveguide feed, similar to how the CEM model was built using a waveport excitation.

For the MVG SGH820 comparison simulation, a high-fidelity model was created as shown in Figure 11 and modeled using the CST FIT algorithm. This model features a coax-to-waveguide adapter feed section of the waveguide, but omits a short section of coaxial transmission line representing the field-replaceable SMA connector. This component is a significant contributor to the ohmic loss of the antenna. To take into account the effect of the SMA style coax connector, the insertion loss of the coax portion only was measured (back-to-back configuration) and subtracted off to determine the IEEE



(a)



(b)

Fig. 10. Comparison of measurement and simulation of the SA Model 12-8.2 serial No. 1, with measurements from (a) NIST in 1992 and (b) NPL in 1991.

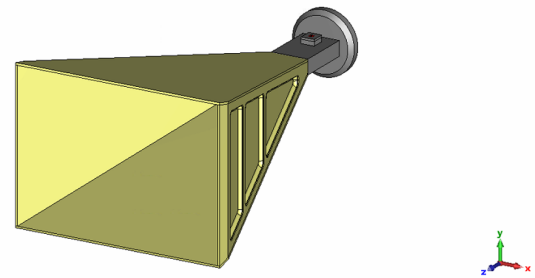


Fig. 11. Picture of high fidelity simulation model of the MVG820 in CST.

gain value. As mentioned previously, an important feature of the horn design is the aperture edges. Due to fabrication process of the SGH820 horn, the edges for the E-plane and H-plane are not identical. The H-plane edges are flat edge and beveled from thick aluminum plates, while the E-plane edges are square-cut from thin sheets (refer to Figure 3). The MVG SGH820 also has exterior ribs on the sides of the antenna which are machined out of aluminum as well as a mounting plate at the back of the coax-to-waveguide transition. These features were added for completion to make the model as close



to the measured horn as possible, but the effects of these minor details were not studied.

Taking all of this into account, the comparison using the MVG SGH820 for measurement versus CEM simulation is plotted in Figure 12. In this case, the agreement between simulated and measured results is within  $\pm 0.08$  dB.

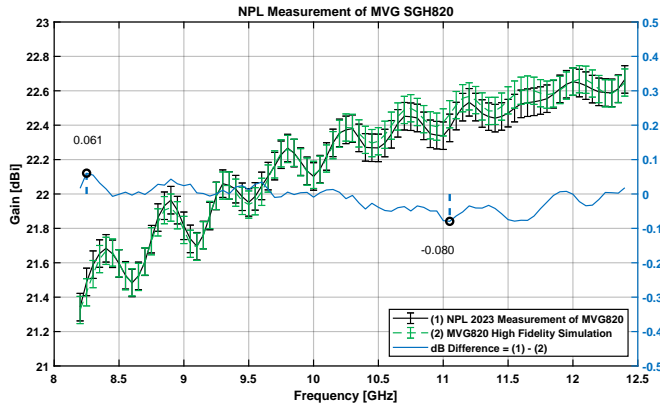


Fig. 12. Comparison of measurement and simulation with the CST FIT algorithm for high fidelity model of the MVG SGH820.

## VI. CONCLUSION

This paper presented the comparison between measurements and simulations of two COTS X-band SGH antennas, the SA Model 12-8.2 and the MVG SGH820, building upon the previous work where inter-code comparison demonstrated a high level of CEM modeling accuracy [1]. Attempts were made to ensure the CEM models matched the physical models as closely as possible. If the geometry is known perfectly, then the error in the modeling is  $\pm 0.0075$  dB. In practice there are build tolerances, however. The uncertainty from the build tolerances of the COTS SGH were determined to be  $\pm 0.0781$  dB and the total RSS uncertainty of the simulation modeling was  $\pm 0.0791$  dB.

Standard practice is to assume SGH on-axis gain is described by the NRL gain curves [3]. When comparing the simulation curve to its corresponding NRL curve, a maximum difference of  $\pm 0.16$  dB was shown. This uncertainty bound is applicable when the physical dimensions of the antenna are absolutely known, particularly the horn length.

Considering the RSS Uncertainty from Table III and assuming no additional knowledge of the as-built horn dimensions, the maximum error in antenna gain normalization based on the appropriate NRL curve is expected to be  $\pm 0.239$  dB. This value is remarkably close to Slayton's 1954 prediction of  $\pm 0.3$  dB for an absolute maximum uncertainty bound, which is the value most commonly used in practice.

Comparing the measured and simulation data for the SA 12-8.2 SGH, the simulated gain is almost always above the measured gain. A maximum and minimum delta of 0.005 dB and -0.149 dB, respectively, was shown for the 1992 NIST measurements and -0.027 dB and -0.166 dB, respectively, for the 1991 NPL measurements. The authors consider this

agreement to be respectable, especially considering we used nominal dimensions for a horn with as-built dimensions that were not available.

Since it is difficult to know the differences between the measurements and the models for the legacy SA horns, a high-fidelity model of the MVG SGH820 was created and compared to measurements performed at NPL in 2023. Taking into account the connector losses, the simulation and measurement fall within each other's error uncertainty bounds. A maximum and minimum delta of 0.06 dB and -0.08 dB was shown. This result is quite good, comparable to the published uncertainties of calibration laboratories.

Based on the results presented here, we expect that careful CEM modeling of SGH on-axis gain can yield comparable uncertainties to measurements performed at national standards laboratories. To complete the uncertainty assessment for the most common SGH configuration, future work will focus on characterizing the uncertainties of common coax-to-waveguide adapters. Additional effort can be made to improve the manufacturing tolerances on a high-fidelity standard gain horn to achieve on-axis gain uncertainties that approach the limits of commercial EM solvers.

## ACKNOWLEDGEMENT

The authors would like to thank Raffaele Scuderi for his contributions towards the simulations with the CST Studio Suite®. We also give a very special thanks to the late Edwin "Ned" Barry, who was initially involved with this paper and provided historical details of the SA Model 12-8.2 SGH.

## REFERENCES

- [1] A. Giacomini, F. Saccardi, L. J. Foged, D. Belgiovane, and J. Dobbins, "Antenna gain calibration with improved accuracy modeling of pyramidal standard gain horns," in *2022 Antenna Measurement Techniques Association Symposium (AMTA)*, 2022, pp. 1–6.
- [2] S. A. Schelkunoff, *Electromagnetic waves*. D. van Nostrand, 1943.
- [3] W. T. Slayton, "Design and Calibration of Microwave Antenna Gain Standards," US Naval Research Laboratory, Washington DC, Tech. Rep., 1954.
- [4] C. Stubenrauch, A. Newell, A. Repjar, K. MacReynolds, D. Tamura, F. Larsen, J. Lemanczyk, R. Behe, G. Portier, J. Zehren, H. Hollmann, J. Hunter, D. Gentle, and J. de Vreede, "International Intercomparison of Horn Gain at X-band," *IEEE Transactions on Antennas and Propagation*, vol. 44, no. 10, 1996.
- [5] IEEE Std 149-2021 (Revision of IEEE Std 149-1979), "IEEE Recommended Practice for Antenna Measurements," 2022.
- [6] J. Nye and W. Liang, "Theory and measurement of the field of a pyramidal horn," *IEEE Transactions on Antennas and Propagation*, vol. 44, no. 11, pp. 1488–1498, 1996.
- [7] J. Odendaal, J. Joubert, and M. Prinsloo, "Extended Edge Wave Diffraction Model for Near-Field Directivity Calculations of Horn Antennas," *IEEE Trans. Instrum. Meas.*, vol. 54, no. 6, Dec. 2005.